Sixth International Symposium on Marine Propulsors
SMP'19, Rome, Italy, May 2019

Transitional flow on model scale propellers and their likely influence on performance prediction

Da-Qing Li, Per Lindell and Sofia Werner

SSPA Sweden AB, Göteborg, SWEDEN

ABSTRACT

Transitional flow on three model scale propellers with different blade areas were investigated by model testing and RANS methods. The boundary layer state of blades in open water and behind conditions were studied by the streamline paint test. A RANS method was coupled with an intermittency transition model to predict the flow.

The paint tests show clearly a laminar flow dominance on blades for all the propellers in low Reynolds number (Rn) open water tests. In the high Rn open water conditions, the near wall flow is a combination of laminar, transitional and turbulent flow. In behind conditions (low Rn due to Froude scaling), the amount of laminar flow is decreased and the amount of transitional to turbulent flow is increased. No separation was present on the high blade area propellers.

We observed that two factors can lead to an unexpected decrease of relative rotative efficiency η_R for low blade area propellers when following the recommendation by ITTC-78 method: (1) The flow separation on the suction side near T.E. in a self-propulsion test that results in a higher torque in the behind condition; (2) A slightly lower open water torque derived from an open water test carried out at a high Rn. The phenomenon is probably more related to the chord length, blade section profile and chordwise load distribution of a propeller design.

Keywords

Reynolds number, laminar/transitional/turbulent flow, scale effects, transition model.

1 INTRODUCTION

The "1978 ITTC performance predication method" (ITTC-78 method in short) has been used for four decades. The method works well in most cases. However, when applied for propellers designed with non-conventional design philosophies, e.g. propeller with extremely low blade area ratios, unusual radial and chord wise load distributions, unusual sections shapes and tip fins of various types the scaling method encounters new challenges with regard to the Reynolds number (Rn) scaling procedure. This paper pays special attention to the low blade area propellers, where a drop of the relative rotative efficiency η_R is sometimes encountered when using the ITTC-78 method. If the drop of η_R is not physical but due to a too simple Rn-scaling scheme, it will lead to an unfavorable full-scale performance prediction. A number of investigators, for example, Tamura and Sasajima (1977), Tsuda et al. (1978) and Hasuike et al. (2013, 2016 and 2017) have attributed this phenomenon to a Rn number difference (i.e. Reynolds scale effects) between the propeller open water test (POT) and the self-propulsion test (SPT) that causes a difference in boundary layer flow between the two tests. Due to the low operational speed of the model ship and the model propeller during a SPT test (Froude's law required) substantial amount of laminar flow may have been developed on propeller blades. For this reason, an alternative scaling method, called "2POT method", was proposed and used by a few ITTC member organizations. It consists of performing two sets of POTs, one at a low Rn equal to the Rn during a SPT test; and the other POT at an as high as possible Rn. The low Rn POW data is used to analyse the SPT results (i.e. determining wake fraction w_{Tm} and relative rotative efficiency η_R etc.) whereas the high Rn POW is used to scale the POW to full scale. The rest of the 2POT scaling procedure for ship powering performance still follows the ITTC-78 method.

Apart from the 2POT method, there are also other scaling methods for POW of conventional propellers that have been developed and are being tested. For instance, the methods by Streckwall et al. (2013, 2016), and by Helma (2015). Lücke and Streckwall (2017) applied paint test on three model propellers in behind and open water conditions to visualise the boundary layer flow structure on blades. The scaling issue and propulsion performance method were discussed accordingly. They found a high amount of laminar flow on all propellers in POT and SPT conditions at a Rn number corresponding to SPT condition. They also noted the streamline orientation in the SPT condition has a more gradual change as in contrast to a sharp separation zone in the POT condition. Analyses of Rn scale effects and scaling methods for ducted propellers and other non-conventional propellers have been addressed by Bhattacharyya1 et al.

(2015, 2016a and 2016b), Sánchez-Caja et al. (2014), Shin and Andersen (2017), and Amadeo et al. (2017), respectively.

The most relevant work in use of transition model for analysis of propeller flow is due to Hasuike et al. (2013, 2016 and 2017) where the authors applied a laminar-kinetic-energy based k-k_L-ω model to determine the laminar flow on many low blade area propellers and compared with available experiment data. The results demonstrated the presence of large amount of laminar flow on blades in open water and behind conditions when the propeller is operated at low Rn numbers. Baltazar et al. (2017) employed a γ-Re_θ transition model to predict POW performance of a conventional and a high-skew propeller in model scale and compared the results with that by model test and a SST k-ω model. Improvement on transition models is still an ongoing topic, as e.g. by Colonia et al. (2017) and Lopes et al. (2017).

In the standard ITTC-78 method, the POT shall be carried out at an as high Rn number as possible and the Rn should, in any case, be greater than the critical transition Reynolds number Rnc. (normally considered to be Rnc ≈ $3x10^5$). During a self-propulsion test where Froude scaling must be applied, the ship and the propeller model are operated at rather low speeds. Typically, the Rn based on sectional chord length at nominal radius 0.75R (R is the propeller radius) is limited to a range of 1~3 $x10^5$. Obviously, there is a difference in Rn between the POT and the SPT, yet the difference is moderate and still within the same order of magnitude (10^5). This difference is much smaller than the Rn difference between a model scale (10^5) and a full scale propeller (10^7). One question is how large Rn scale effect will be introduced with this moderate difference for model scale propellers? Would different propellers react to this Rn difference differently? Operating a propeller at a Rn number lower than Rnc would imply the occurrence of laminar flow and possibly flow separation. However, there is a counteracting effect on the propeller in behind condition where the ship wake contains a high level of turbulence intensity, making the propeller more prone to develop a turbulent flow on blades. One would wonder how large blade area is actually covered by laminar flow in a SPT and what is the difference in the boundary layer characteristics for a propeller operating in behind condition and in open water condition at a same Rn? What is the reason for the unexpected low η_R value and what type of propellers have such an issue?

The paper attempts to address these questions by means of model testing method, assisted by a RANS method coupled with a transition model to investigate the boundary layer flow over the propeller blades. POT test and streamline paint test were conducted for three propellers at a low and a high Rn number. The chosen propellers represent a modern low blade area high efficiency propeller (of NAKASHIMA design), and two conventional designs with a medium and a high blade area respectively. Paint test was also performed in behind condition for these propellers to look at the difference in the near wall boundary layer flow. Some comments are made on the 2POT method.

2 PROPELLER MODEL AND MODEL TEST

The propeller particulars are presented in Table 1, in which R is the propeller radius and $t_{max}/C_{0.75R}$ is the maximum thickness-to-chord ratio at 0.75R radial section.

In a POT, the propeller model is mounted on a horizontal shaft and towed through the water at an immersion of the shaft centre equal to one propeller diameter. During the test, the rate of revolutions is kept constant whilst the advance speed is varied to achieve a series of advance ratios (J). A hull model, originally fitted to Prop A, is used for the other two propellers in SPT. The SPT for Prop A was performed at design speed with design draft at J=0.388.

In a streamline paint test, the propeller was mounted in the same way as in POT and SPT, but only one run at one speed was made. Before the test the propellers were painted with black streamline paint at the leading edge (L.E.). The test was performed at a high and a low Rn number for each propeller, according to the loading conditions shown in Table 2. The two Rn:s, based on the relative resultant velocity at 0.75R blade section, are also given in the table. Photographs were taken after each test. The chosen low Rn numbers correspond to a typical Rn used in a SPT.

Table 1 Main particulars of the propellers

Propeller	$A_E/A_0/Z$	$t_{max}/C_{0.75R}$	$C_{0.75R}/D$	No of blades
Prop A	0.10	-	-	-
Prop B	0.13	0.0350	0.27	4
Prop C	0.16	0.0438	0.33	5

Table 2 Loading conditions for POT

	Prop A		Prop B		Prop C	
Cond.	low Rn	high Rn	low Rn	high Rn	low Rn	high Rn
N [rps]	8.1	20	6	18	5	15
V_A[m/s]	1.214	3	1	3	1	3
J [-]	0.646	0.646	0.694	0.694	0.824	0.824
Rn [$x10^5$]	2.06	5.08	2.15	6.46	2.24	6.71

3 NUMERICAL METHODS

3.1 Numerical models

The viscous flow is solved by an incompressible Reynolds Averaged Navier-Stokes (RANS) method using ANSYS FLUENT 18.2. Menter's Shear Stress Transport (SST in short) k-ω turbulence model (Menter 1994) is

employed for simulation of fully turbulent flow, serving as a reference for comparison with the transition model.

3.2 Transition model

The intermittency transition model, γ-model, is a further development of the γ-Re_θ model, based on the coupling with SST model with a transport equation for turbulence intermittency γ (hence a 3-equation model). It inherits the same underlying modelling concept as the γ-Re_θ model, e.g., local-correlation based transition modelling, and the correlation between transition phenomena and free stream turbulence intensity and pressure gradient. The detail is referred to Menter (2015). The model has an option for cross-flow transition, which is used in the present work.

3.3 Numerical schemes are as follows

- Incompressible pressure-based solver.
- Pressure and velocity solved in a coupled manner.
- 2nd order discretisation for pressure gradient at face.
- QUICK scheme for all transport equations.
- SRF for POT calculation in steady mode.
- Sliding mesh grid interface for calculation in behind condition in unsteady mode.

3.4 Boundary conditions (BC)

Constant velocity, turbulence intensity (*Tu*) and turbulent viscosity ratio (*TVR*) are specified at the velocity inlet boundary, whereas a zero pressure is set at the outlet boundary. No-slip wall is set on all body surfaces. It is well known that transition models are sensitive to the turbulence quantities prescribed at the inlet. A number of turbulence quantities were tested and compared with model test result in the initial study. The adopted values, presented below, are a compromise that gives reasonable agreement with the paint test results and the measured POW data.

For simulation in POT condition, the turbulence quantity at velocity inlet is set as, *Tu*=2%, *TVR*=6, intermittency γ=1 (for γ–model). For simulation in behind conditions, the free surface, side and bottom boundaries are treated as symmetry plane. The turbulence quantity at velocity inlet is prescribed as, *Tu*=5%, *TVR*=10, and γ=1.

4 COMPUTATIONAL DOMAIN AND MESH

For simulation in POT condition, the CFD domain consists of a blade passage by utilizing the circumferential periodic BCs and single rotational reference frame (SRF). The distance of the domain boundaries to the centre of propeller are defined as a multiple of propeller diameter *D*. namely, Inlet = 2D, Outlet = 3D, Outer radial = 3D. The meshes generated on the two periodic surfaces are fully conformal. All meshes are of hexahedral type. The non-dimensional wall-normal distance (y^+) of the 1st cell layer to the blade surface is kept below 1. Figure 1 shows the CFD domain for the calculations in open water conditions.

For simulation in behind condition (only with Prop A), the domain is a rectangular box. The distance of the domain boundaries is defined as a multiple of ship length Lpp as follows: Inlet = 0.7Lpp, Outlet = 2Lpp, Sides = 1Lpp from central plane, Bottom = 1Lpp from free surface level.

The mesh for the computation in behind condition is generated by HexPress. The mesh on blades is refined in the wall-normal direction to achieve a $y^+<1$ whereas the near-wall distance to hull surface is set to a $y^+ = 2$. The mesh count for the simulations is given in Table 3. Figure 2 shows the surface mesh on the suction side (SS) of the blade for each propeller.

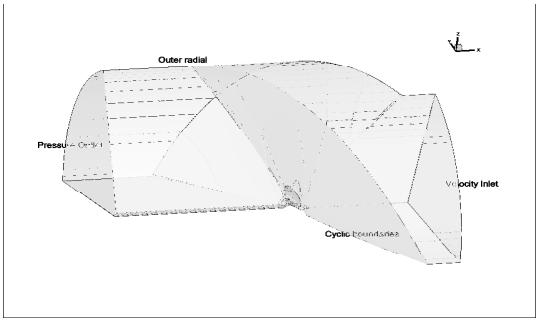

Figure 1 Computational domain for the POT calculations

Table 3 The mesh count for simulations

Propeller	A	B	C	A (behind)
No of cells [million]	5.028	3.840	4.091	8.193

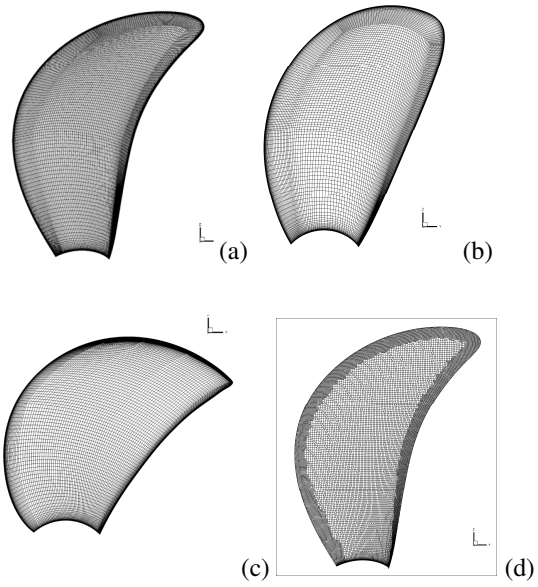

Figure 2 Surface mesh on the suction side of Prop A (a), Prop B (b), and Prop C (c) and Prop A in behind condition (d)

5 RESULTS AND DISCUSSIONS

Computational results are compared with available model test data with regard to the near-wall boundary layer flow, the pressure and skin friction coefficients along blade sections, and the POW curves in the following subsections.

5.1 Convergence of solution

The flow solver has a stable convergence behaviour in this work, and none of the computations encountered a divergence problem. The steady computations were run generally for about 8000 iterations. An example convergence history for a POT calculation with γ-model and SST model is given in Figure 3. As seen in Figure 3, the residuals for all the equations have dropped to a level below 10^{-4}, the iterative solution is considered well converged after 8000 iterations.

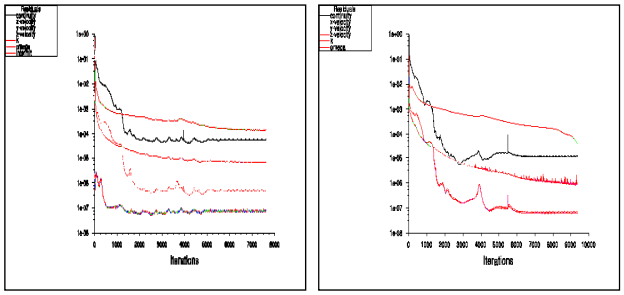

Figure 3 Convergence of γ-model (left) and SST model (right)

5.2 In open water conditions

5.2.1 Paint test vs. predicted near wall flow

In following figures, paint test results are presented in the 1st row, contour plot of skin friction coefficient Cf overlaid by limiting streamlines, is presented in the 2nd row. The contour of turbulence intermittency γ in the range of [0.02 0.08] is displayed in the 3rd row. The limiting streamlines by SST model is shown in the 4th row. In a paint test, the flow direction of paint is governed by the force balance between the skin frictional and centrifugal forces. For blade area with fully laminar flow where the frictional force is relatively low and the centrifugal force is dominant, the traces of paint will predominantly go in the radial direction on blades. For blade area with fully turbulent flow where the frictional force is large and dominant over the centrifugal force, the paint traces will solely follow the circumferential lines. The turbulence intermittency of a value equal to or less than 0.02 is used for laminar regimes according to ANSYS Fluent, so any dark blue areas with $\gamma \leq 0.02$ implies a laminar zone. The value in the range γ = [0.02 0.08] corresponds roughly to the transitional zone from laminar to turbulent flow. Values above 0.08 can be regarded as turbulent flow.

Prop A

For Prop A, the RANS results are compared with the photos of the paint test in Figure 4 for the low Rn and Figure 5 for the high Rn condition. In the low Rn condition (Figure 4), the paint test reveals a strong radially-going flow on both side of blades, indicating a status of laminar flow. Near the T.E. on the suction side (SS), the radially-going streamlines are concentrated at ca 0.8C chordwise location, indicating an occurrence of flow separation. A very similar pattern is reproduced by the γ-model. A transitional zone is visible on the SS near the T.E. and near the root on the pressure side (PS) for Prop A. The streamlines predicted by SST model show also a good agreement with the paint test on SS, but are somewhat different from the experiment on PS near the root and tip region: they exhibit a more tangentially going flow.

In the high Rn case (Figure 5), the paint test shows that the flow is directed more in the circumferential direction, especially at the outer radii SS, indicating the expected turbulent flow structure. It is unclear in the photo whether there is a separation near T.E. on SS. A large discrepancy is seen for the γ-model which computed more radially-oriented streamlines on the PS. This means that the laminar flow region is overpredicted. On the SS close to T.E region, a strong radially-going flow and a flow separation along the T.E. are predicted by the γ-model, but no separation can be verified from the paint test result. In the outer blade area (0.75R< r <1.0R), the paint test indicates a fully turbulent flow whereas the γ-model exhibits an overpredicted laminar flow on the SS. Compared with the γ-model, SST model seems to have a closer agreement with the experiment.

Prop B

Limiting streamlines on Prop B are compared with the paint test results in Figure 6 for the low Rn case and in Figure 7 for the high Rn condition.

In the low Rn POT case in Figure 6, the paint test reveals that the flow is going in the radial and tangential direction on both sides. Separation occurs on the SS at a distance upstream the T.E. and the separation line is parallel to the T.E.. This concentration of streamlines is well captured by the γ-model and SST model, the latter model gave a somewhat different pattern between the concentration line and T.E. The streamlines show a slightly stronger radial orientation than the paint test traces. The models also predicted a reattachment along the L.E. on the PS. The intermittency quantity γ shows a transitional flow on large part of PS and a laminar flow on SS.

In the high Rn condition (Figure 7), the streamlines on the inner blade area (with r < 0.65R) still have a radially orientated velocity component. The flow on the outer blade area, after a short transition distance from the L.E., turns quickly to tangential (turbulent) flow. The intermittency contour plot shows a high amount of transitional/turbulent flow on the PS. There is about 40% transitional and 60% laminar flow on the SS. Compared with SST model, the γ-model gives better agreement with the paint test on the SS.

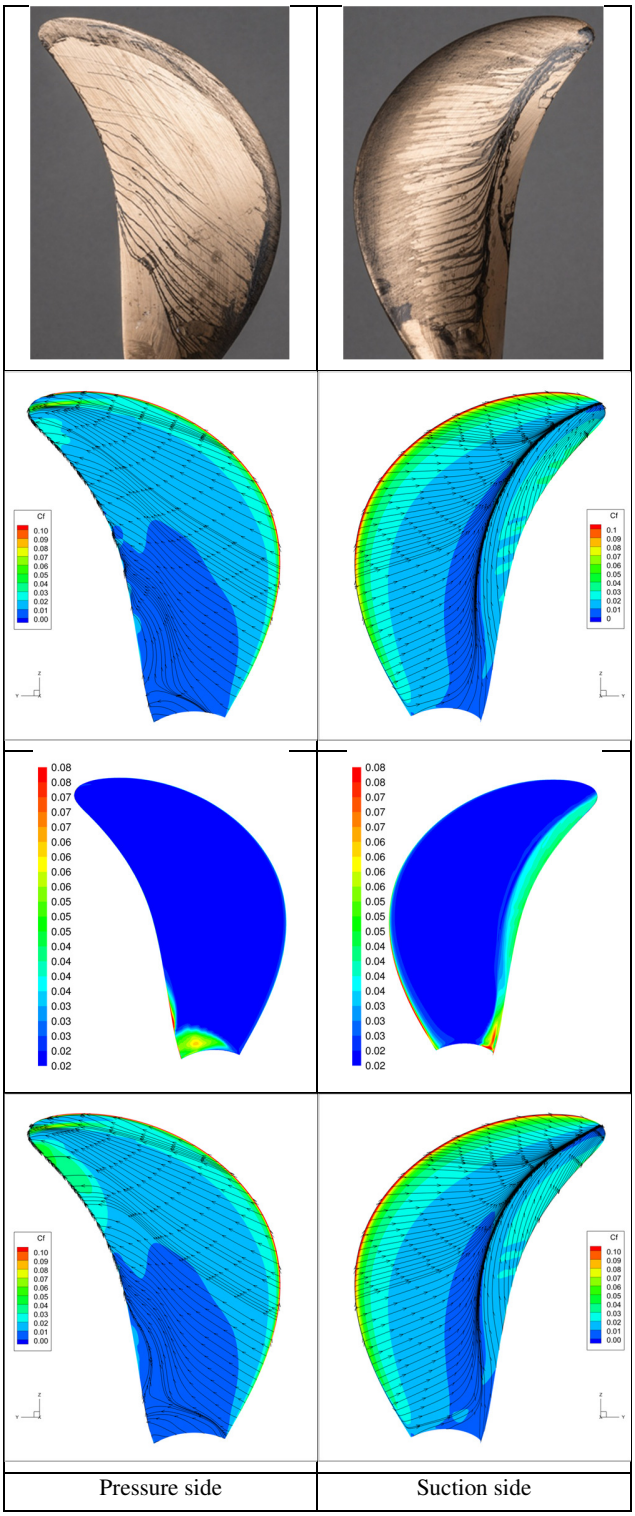

Figure 4 Prop A at low Rn. Paint test vs. limiting streamlines by γ-model (row 2), turbulence intermittency (row 3) and limiting streamlines by SST model (row 4)

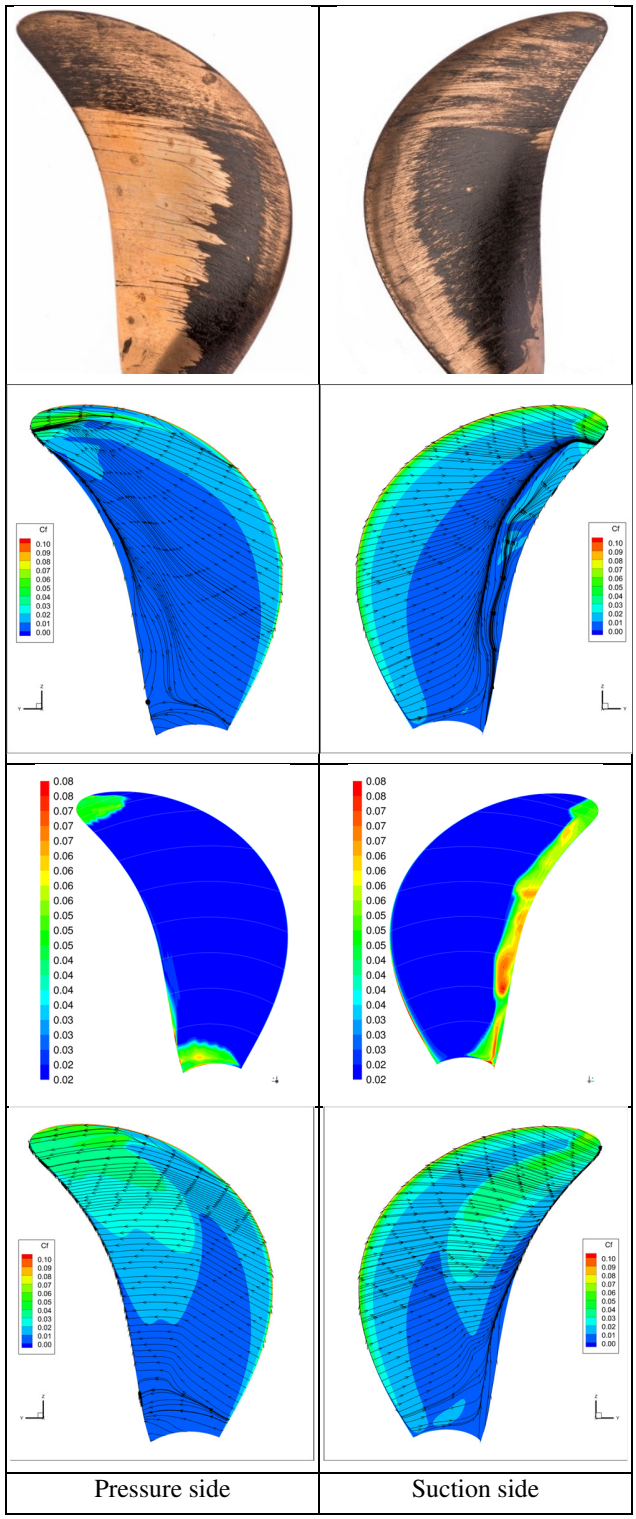

Figure 5 Prop A at high Rn. Paint test vs. limiting streamlines by γ-model (row 2), turbulence intermittency (row 3) and limiting streamlines by SST model (row 4)

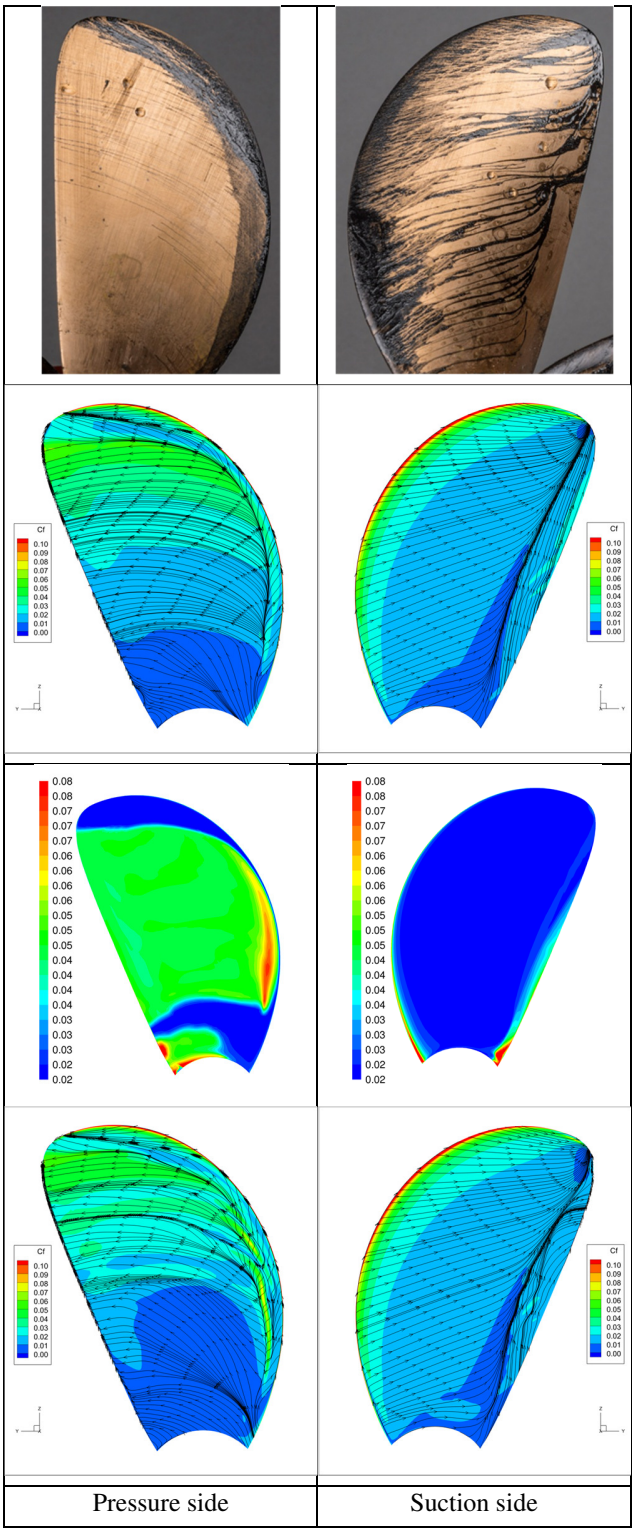

Figure 6 Prop B at low Rn. Paint test vs. limiting streamlines by γ-model (row 2), turbulence intermittency (row 3) and limiting streamlines by SST model (row 4)

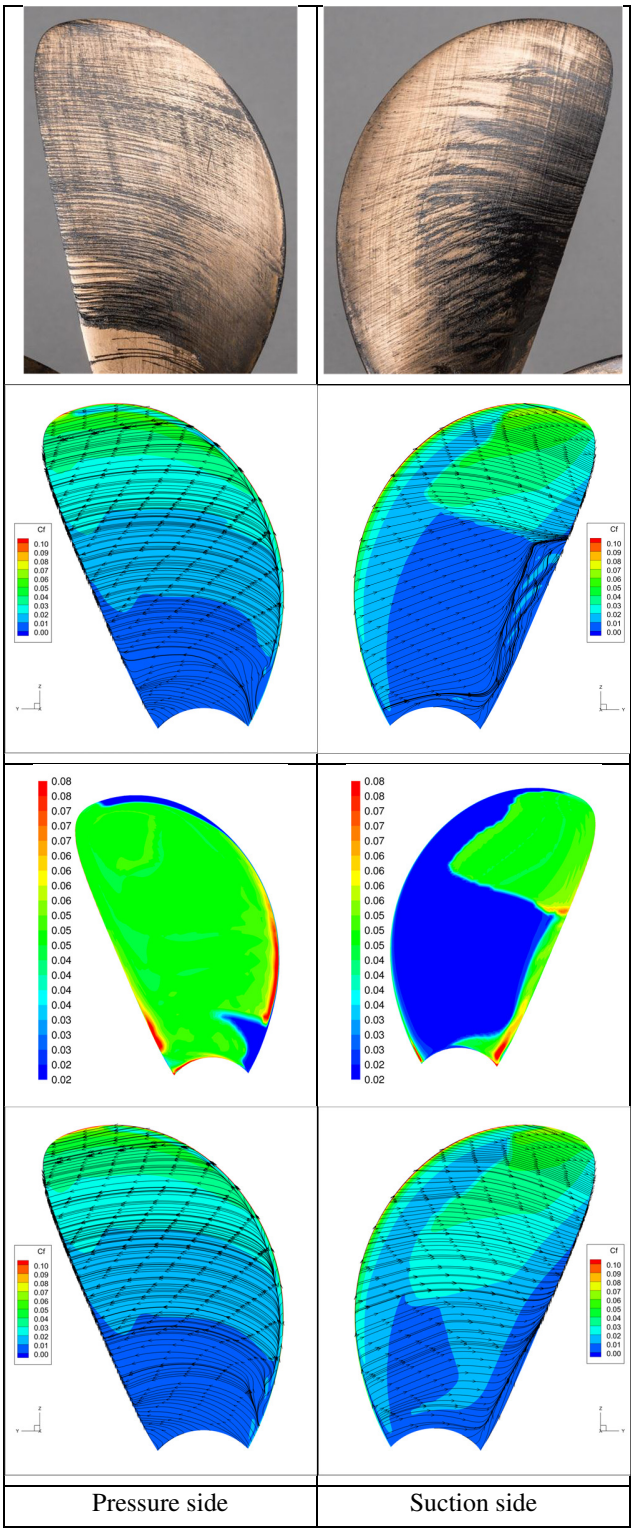

Figure 7 Prop B at high Rn. Paint test vs. limiting streamlines by γ-model (row 2), turbulence intermittency (row 3) and limiting streamlines by SST model (row 4)

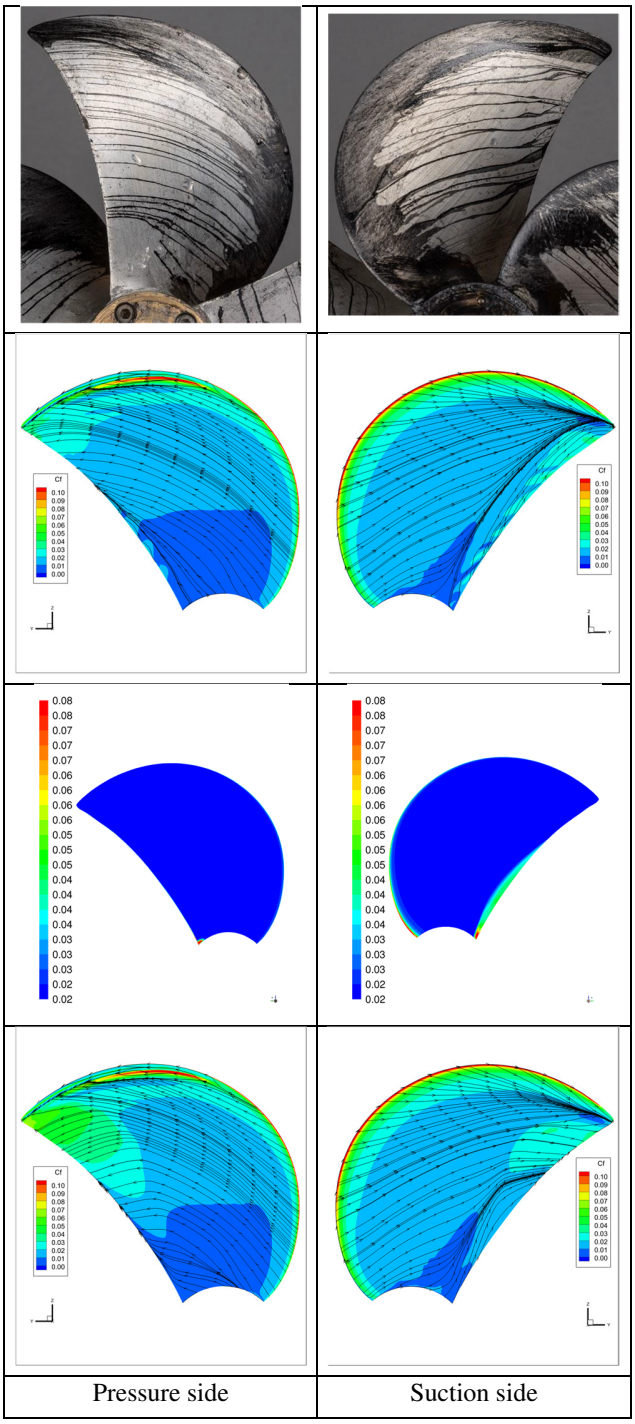

Figure 8 Prop C at low Rn. Paint test vs. limiting streamlines by γ-model (row 2), turbulence intermittency (row 3) and limiting streamlines by SST model (row 4)

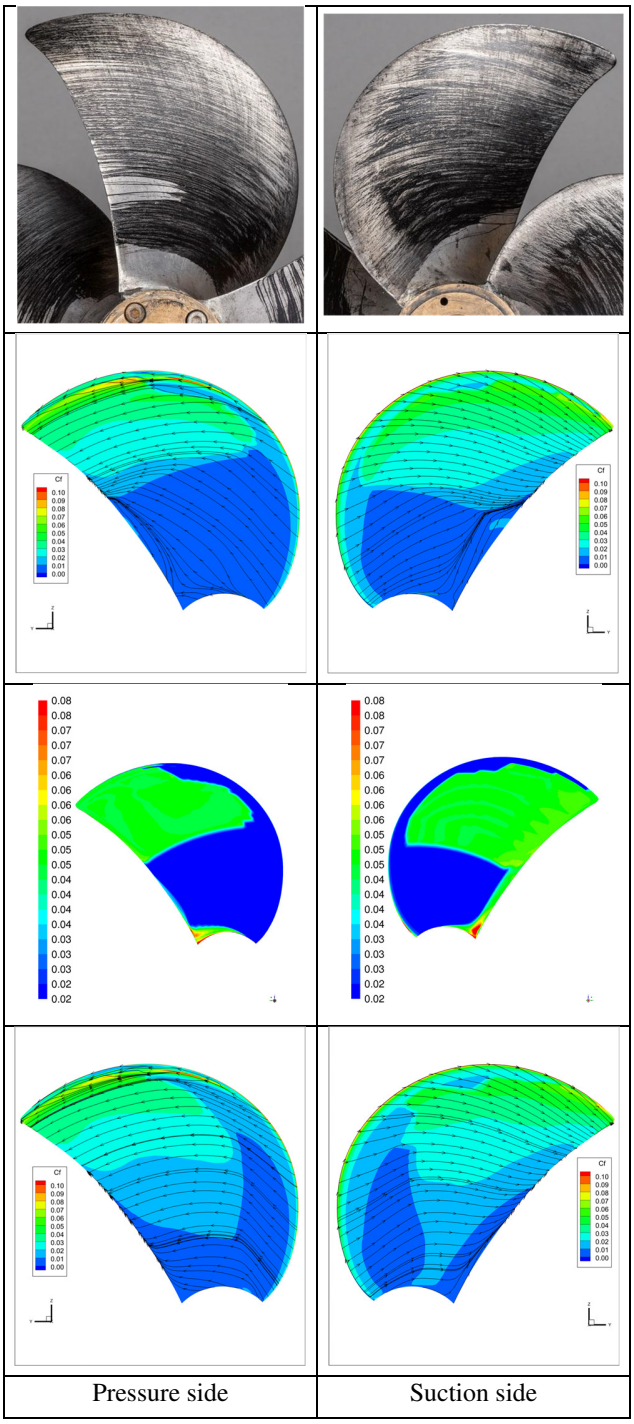

Figure 9 Prop C at high Rn. Paint test vs. limiting streamlines by γ-model (row 2), turbulence intermittency (row 3) and limiting streamlines by SST model (row 4)

Prop C

Limiting streamlines on Prop C are compared with the paint test results in Figure 8 for the low Rn case and in Figure 9 for the high Rn case.

At low Rn, the paint traces imply a mixture of laminar and transitional flow on both sides. On the SS there are a few traces of flow separation before the flow reaches the T.E.. Compared with the paint test, the limiting streamlines by the γ-model demonstrate a stronger radial orientation, meaning

that the laminar part is over-predicted. This can also be seen from the intermittency contour plot (being entirely blue) in Figure 8. The streamlines by SST model exhibit some more transitional flow content near the T.E. on the outer blade. Both models predicted flow separation on the SS near the T.E., but the separation line predicted by SST model is a bit shorter than that by the γ-model.

At the high Rn, more tangentially going streamlines are observed from the paint test, particularly on the PS. At the inner radii on the SS starting from the L.E., some streamlines show a radial velocity component, indicating a region of laminar flow. The limiting streamlines predicted by the γ-model are oriented more to the radial direction at the inner radii, showing a dominance of laminar flow on the inner blade surface, whereas those predicted by the SST model appear to have closer agreement with the experiment. On the outer blade area, both models and the paint test suggest a fully developed turbulent boundary layer.

To summarise the prediction by the γ-model: at low Rn, the agreement with the paint test result is fairly good for Prop A and B, but over-predicted laminar zone for Prop C; At high Rn, the agreement with the paint test is good for Prop B, but less satisfactory for Prop A and C where an overestimation of laminar flow is noted. Flow separation appears to be slightly over-predicted too for all propellers at high Rn. The flow predicted by the SST model are similar with the γ-model for the low Rn cases, but the Cf is probably overestimated. For the high Rn cases, the streamlines in the transition to turbulence region correspond fairly well with the paint traces. The separation region predicted by the SST model is less than that by the γ-model.

5.2.2 Flow feature along blade sections

The pressure coefficients -Cp at blade section r=0.5R and 0.7R, predicted by the γ-model in the low Rn case, are compared for Prop A and Prop C in Figure 10 and Figure 11. The skin coefficients Cf at these sections are compared in Figure 12 and Figure 13.

The non-dimensional chordlength (x/C) of Prop C is rescaled along the abscissa relative to Prop A, to show a chord length relationship with Prop A. The K_T for Prop C is a bit higher than Prop A, meaning that the sectional loading on Prop C is higher than Prop A. However, looking at the downstream part of Cp curves for the two propellers in Figure 10 and Figure 11, it is clear that the adverse pressure gradient on the suction side (SS) of Prop A is relatively higher than Prop C. This is a rather significant difference between Prop A and C: it implies that Prop A is more prone to flow separation, particularly in the case when the blade is working in a laminar flow that is highly sensitive to disturbance. Severe separation can be confirmed from the paint test streamlines for Prop A but not for Prop B (Figure 4 and Figure 8). No laminar separation bubble can be verified since the typical pressure plateau caused by laminar separation bubble is not present on the Cp curves. From the Cf curves in Figure 12 and Figure 13, one can speculate that the transition onset starts at a chordwise location approximately at x/C≈ 0.70 for Prop A and x/C≈ 0.82 for Prop C.

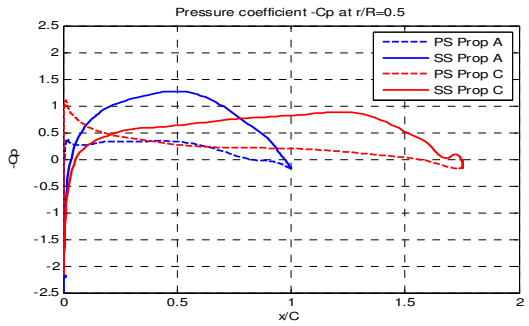

Figure 10 -Cp comparison at 0.5R for Prop A and C

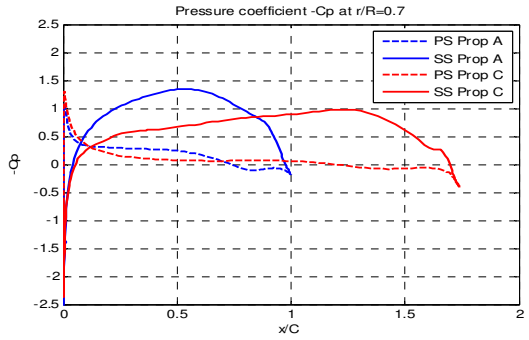

Figure 11 -Cp comparison at 0.7R for Prop A and C

5.3 In behind condition

Paint tests of the propeller fitted to a ship model were conducted for all propellers but CFD computation was performed only for Prop A. It should be mentioned that the paint traces from paint test in a SPT represent an averaged boundary layer flow characteristics resulting from many number of blade revolutions through an inhomogeneous wake.

5.3.1 Paint test results and predicted streamlines

The paint test results for Prop A are compared with the limiting streamline predicted by the γ-model and SST model (the 4th row) in Figure 14. Firstly, we noted from the paint test that the near wall flow is still dominated by a radially-oriented flow, similar yet different from that in the low Rn open water case (Figure 4). Such characters were also reported by Hasuike et al. (2017) and Lücke et al. (2017). The near wall flow pattern in behind condition is much more complicated, due to a variable angle of attack to blade sections in the radial and circumferential directions, a high turbulence level in the ship wake. The high turbulence intensity might have stabilised the flow to just delay or avoid a separation, but is not sufficient to change the boundary

layer character from laminar to fully turbulent, so the blade is still covered with a mixture of laminar and transitional flow, as seen from the paint test results. It is however unclear whether separation took place on the SS for Prop A.

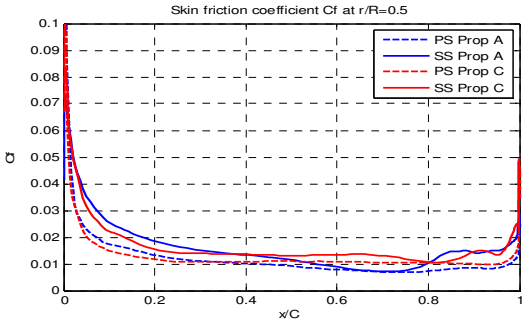

Figure 12 Cf comparison at 0.5R for Prop A and C

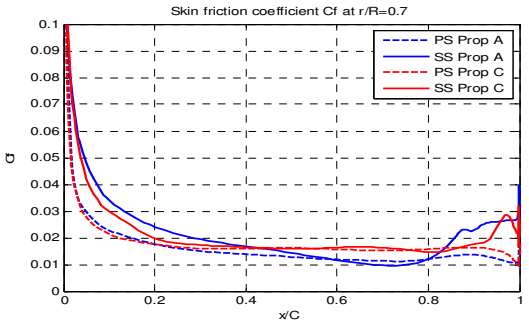

Figure 13 Cf comparison at 0.7R for Prop A and C

The γ-model predicted a more laminar flow content on the outer part of the blade than the paint test. On the inner part of the blade, the trend is just the opposite. The streamlines predicted by the γ-model exhibit a less extent of radial orientation compared with the paint test, indicating an under-estimation of laminar flow and an over-estimation of transitional/turbulent flow. This behaviour can be also seen in the contour plot of intermittency (3rd row) in Figure 14: the amount of transition/turbulent flow area is increased significantly in the SPT, compared with that in POT case (Figure 4). The high γ value (red area) suggests that a part of flow has turned into turbulent, but this character does not agree with the paint traces.

Both models predicted a flow separation near and parallel to the T.E., as implied by the converging streamlines in Figure 14. The γ-model also predicted a L.E. vortex separation and subsequent reattachment along the L.E. at the outer radii.

The paint test results for Prop B and C are presented in Figure 15, and they are compared with the respective open-water cases in Figure 6 to Figure 9. For Prop B, starting from L.E. a laminar flow develops and covers about half of the blade area, then the flow gradually changes direction towards more circumferential, indicating a transitional state of the flow. However, unlike the open water case, no separation is observed in the behind condition.

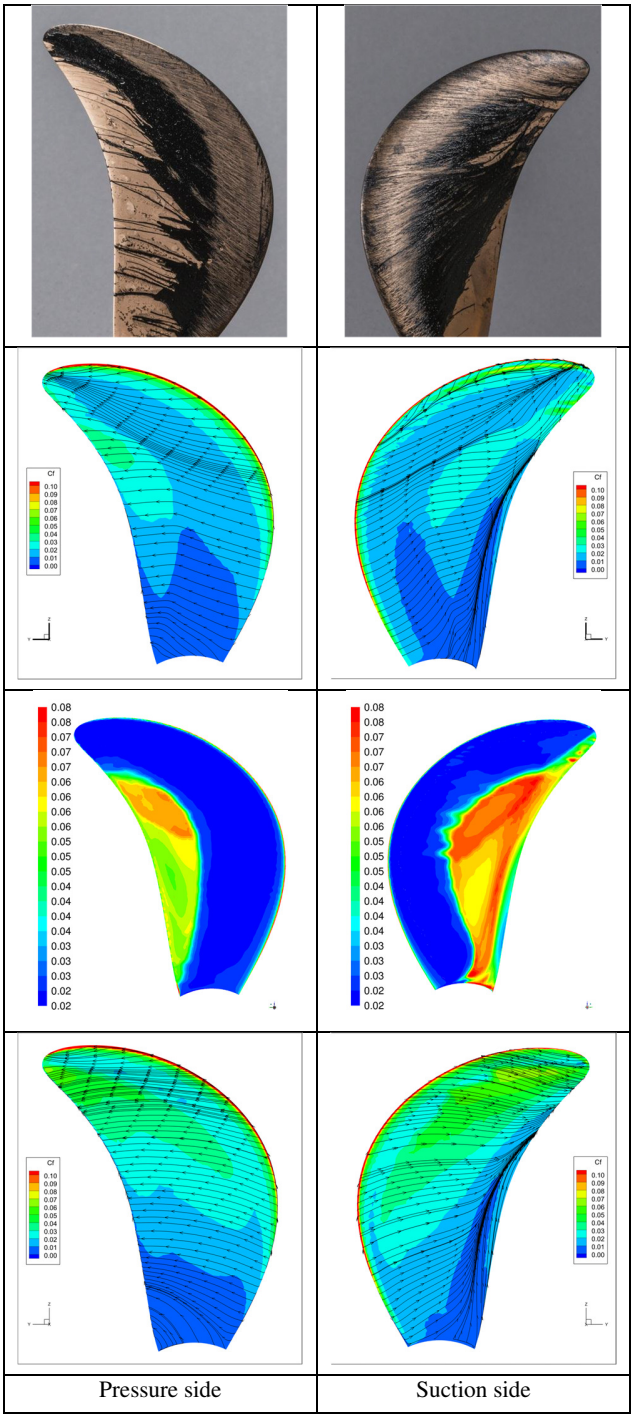

Figure 14 Prop A in behind condition. Paint test vs. limiting streamlines by γ-model (row 2), turbulence intermittency (row 3) and limiting streamlines by SST model (row 4)

For Prop C, the paint traces have some similarity with those observed in the low Rn open water condition (Figure 8), yet with two discrepancies. They starts with a clear and strong laminar flow pattern from the L.E., spread about 1/4 chordwise over the blade, then the flow direction is changed more to the circumferential one, possibly due to the disturbance of a high turbulence intensity. As a result, the flow over the rest of 3/4 blade area exhibits a transitional flow character. No separation can be found on the SS.

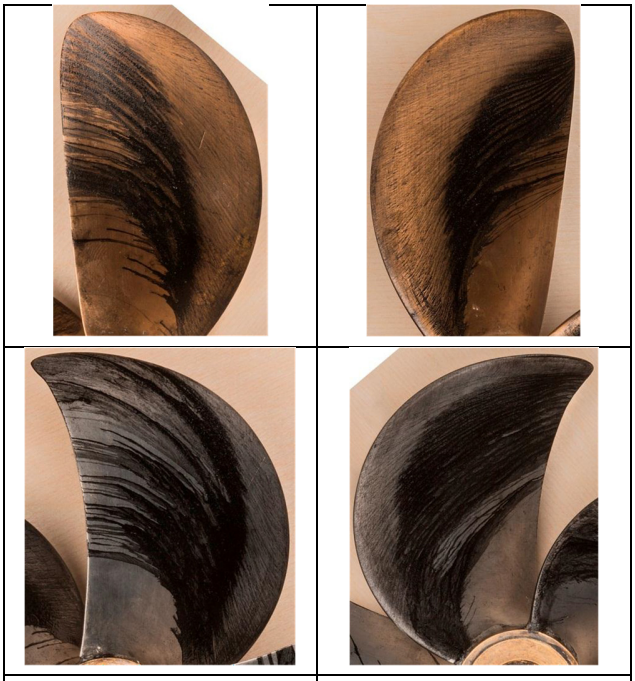

Figure 15 Paint test results for Prop B (top) and C (bottom) in behind condition

5.3.2 Flow feature along blade sections

The pressure (Cp) and skin friction coefficient (Cf) at blade section r=0.7R for Prop A is shown in Figure 16. Compared with the Cf in POT case in Figure 13, it is seen that the transition location is moved upstream to x/C≈0.5 on SS and x/C≈0.65 on PS in the behind condition.

Comparing the studied propellers in behind condition, we noted that the near wall flow is still dominated by laminar and transitional flow, but with a decreased amount of laminar and an increased amount of transitional flow, compared with the open water cases at low Rn. For the two high blade area propellers (B and C), there is no separation on SS. Although separation cannot be verified for Prop A from the present paint test result, both the experiment and computational work by Hasuike et al. (2013, 2016 and 2017) have confirmed that flow separation is constantly present in SPT for low blade area propellers. We believe that flow separation in SPT has made a low blade area propeller significantly different from a high blade area propeller. The paint tests carried out at HSVA (Lücke and Streckwall 2017) also confirmed this difference. The high blade-thickness-to-chord ratio and the high adverse pressure gradient near the T.E. for the low blade area propellers have made the blade section more vulnerable to flow separation. It is likely that the flow separation has resulted in an increased pressure drag, thereby leading to a higher K_{Qb} in behind condition. This might have played a role for the unexpected drop of η_R when the standard ITTC-78 method is used. (to be explained further in §5.5)

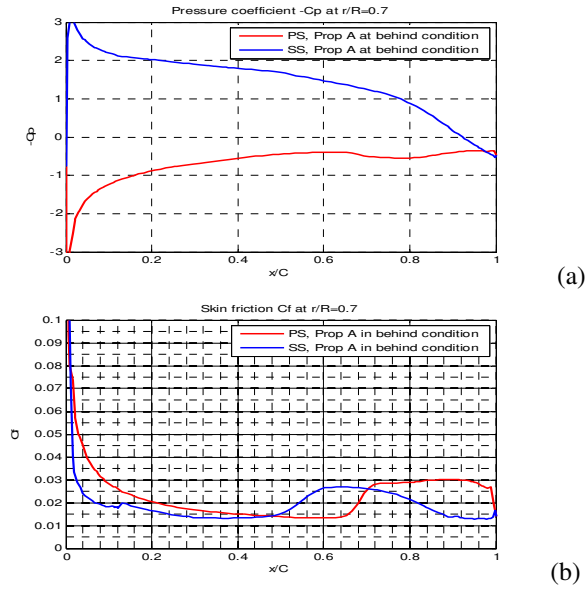

Figure 16 Cp and Cf at 0.7R, Prop A in behind condition

5.4 POW characteristics at two Rn numbers

To show the difference in POW at the low Rn and the high Rn (see Table 2 for the Rn difference), the measured POW data for Prop A, B and C are presented in Figure 17, Figure 18 and Figure 19, respectively.

For Prop A, the K_Q at the low Rn is slightly higher than that in the high Rn case for the low-J values and becomes lower for the high-J range. Difference in K_T only occurs for the high-J values, where K_T at the low Rn is lower. For Prop B, the scale effect occurs mainly for high-J values where both K_T and K_Q at the low Rn are a bit lower than those at the high Rn, a typical sign that the propeller tested in the low Rn case is working below the subcritical Reynolds number. For Prop C, K_Q at the low Rn is higher than that at the high Rn over the range of J<0.6. K_T and K_Q at the low Rn are lower than those at the high Rn for the range with J > 0.6. The response of POW to the Rn difference is obviously propeller design dependent. Different propeller exhibits different extent of scale effect due to a moderate change of Rn. Assuming a propeller is normally operated in an open water efficiency range of $0.5<\eta_0<0.65$ in model tests, the difference in K_T

(and K_Q) between the two sets of POW is not greater than 2.5%. The difference in η_0 can be larger, e.g. for Prop A.

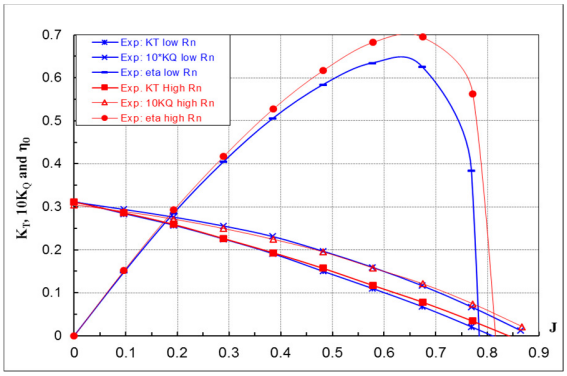

Figure 17 POW of Prop A at low and high Rn

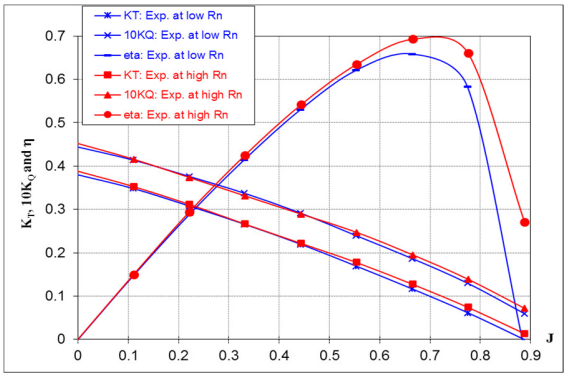

Figure 18 POW of Prop B at low and high Rn

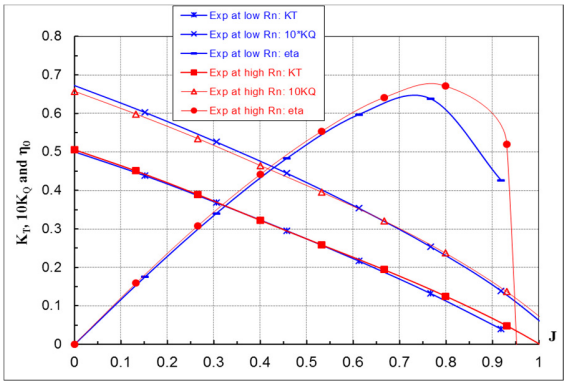

Figure 19 POW of Prop C at low and high Rn

The K_T and K_Q predicted at the same J as the paint tests are presented for the γ-model in Table 4 and for the SST model in Table 5. The error relative to experiment data is also shown in the tables. It is seen that the POW predicted by the γ-model has a closer agreement with the measured data than SST model, as expected. Both models show a tendency to underpredict the K_T and K_Q with a relatively large error than usual. On the other hand, considering that the J value used in these computations lies far off the design J, a larger deviation of computed POW is to some extent expected. For Prop A and B, the prediction errors of the γ-model are larger in the low Rn case compared with the high Rn case. Detail analysis of computational results is beyond the scope of the paper, and will be discussed in another paper.

Table 4 POW predicted by the γ-model

Prop	Rn [x10^5]	J	K_T	10*K_Q	η_o	ΔKT %	ΔKQ %	Δη_o%
A	2.06	0.646	0.077	0.122	0.650	-4.3	-6.3	2.2
	5.08	0.646	0.088	0.126	0.715	-2.7	-4.8	2.2
B	2.15	0.694	0.098	0.169	0.642	-4.5	-2.4	-2.2
	6.46	0.694	0.109	0.179	0.671	-3.6	-1.4	-2.2
C	2.24	0.824	0.099	0.203	0.638	1.4	-3.5	5.1
	6.71	0.824	0.101	0.212	0.627	-9.2	-3.5	-5.9

Table 5 POW predicted by the SST k-ω model

Prop	Rn [x10^5]	J	K_T	10*K_Q	η_o	ΔKT %	ΔKQ %	Δη_o%
A	2.06	0.646	0.072	0.115	0.641	-10.4	-11.3	1.0
	5.08	0.646	0.081	0.122	0.682	-9.8	-7.5	-2.5
B	2.15	0.694	0.103	0.174	0.654	0.4	0.8	-0.4
	6.46	0.694	0.106	0.176	0.665	-5.9	-2.9	-3.1
C	2.24	0.824	0.097	0.203	0.629	-0.3	-3.6	3.5
	6.71	0.824	0.098	0.206	0.626	-12.0	-6.3	-6.0

5.5 Implication on performance prediction

An unusual low value of relative rotative efficiency η_R is obtained when the ITTC-78 method is used in the performance prediction for some propellers, as e.g. reported by Tsuda et al. (1978) and Hasuike et al. (2013, 2016 and 2017). The authors attributed this phenomenon to a Reynolds scale effect caused by the Rn difference between the POT and the SPT. We agree that this could be one reason. However, there might be other reasons too.

In Table 6, the propulsive efficiency factors predicted by the ITTC-78 method, as well as a 2POT method (for Prop A), are presented for a few cases with these propellers used in the SPT. The Rn level used in the POT is marked with low or high. Each case refers to a design loading of a vessel. The n_m in the table is the rate of revolution during SPT.

Table 6 ITTC-78 vs 2POT predicted propulsive factors

Prop	Case	Vs [kn]	POT test at	n_m [1/s]	η_{om}	η_R	η_H	ship η_o	ship η_D
A	1a	14.5	high Rn	8.1	0.540	0.991	1.170	0.614	0.711
	1b	14.5	low Rn	8.1	0.508	1.029	1.180	0.610	0.741
B	2	14	high Rn	6.6	0.575	1.022	1.224	0.631	0.790
	3	14.5	high Rn	7.4	0.592	1.019	1.149	0.634	0.742
	4	15	high Rn	7.5	0.609	1.023	1.145	0.647	0.758
C	5	24	high Rn	8.9	0.657	1.020	1.080	0.689	0.759
	6	22	high Rn	9.6	0.614	1.021	1.119	0.648	0.740

For Prop A, we see in Table 6 (Case 1a) an unusual low η_R (η_R =0.991) is obtained when the ITTC-78 method is used. Using a 2POT method with a POT tested at a low Rn, we see an expected level of magnitude is obtained, i.e. η_R =1.029 (Case 1b). This is the situation with the low blade area propeller. If we now look at the two conventional propeller, B and C, they both are run at about the same low Rn as Prop A during SPTs for all the cases (Case 2-6). POT is run at a high Rn and only the standard ITTC-78 method is applied. In all these cases the predicted η_R have an expected level of magnitude! From the POW curves in Figure 18 and Figure 19 we see that there is also some Rn scale effect on Prop B and C, particularly for Prop C, but why these two propellers do not suffer from the drop of η_R? The answer is probably related to the flow separation phenomenon in SPT for the low blade area propellers, as discussed in §5.3.2. We observed a significant difference between a low and a high blade area propeller from the paint test result in SPT: flow separation is present on the SS of the low blade area propeller but no separation on the high blade area propeller! The separation can lead to a high pressure drag, which reduces the thrust and increases the torque in behind condition, hence leading to a low efficiency η_{om}. The low efficiency value of η_{om} is evidenced in Table 6 for Prop A, as compared with Prop B and C.

There are two factors that can lead to a decrease of η_R. (a) A moderate difference in POW curve due to a Rn difference in a POT and a SPT; (b) Flow separation on blades during a SPT. As per definition, $\eta_R=Q_{m0}/Q_{mb}$ where Q_{m0} is the torque interpolated from the POW curve using K_T-identity method and Q_{mb} is the measured torque in behind condition during the SPT. A minor Rn difference between POT and SPT can give rise to a lower Q_{m0} (by a POW curve from a high-Rn POT) that leads to a decrease of η_R. On the other hand, an unexpectedly high Q_{mb} (caused by flow separation) could also lead to a drop of η_R. Occurrence of flow separation near the T.E. implies a higher pressure drag on blades and hence an increase of Q_{mb}. This will lead to a lower η_R. In reality, it might as well be so that both a higher Q_{mb} in SPT and a lower interpolated Q_{m0} from a POT tested at a high Rn collaboratively result in an unusual decrease of η_R. The two conventional propellers do not suffer from the issue of η_R due to a longer chord length and a gradual change of the adverse pressure gradient towards the T.E. Furthermore, we want to point out that, if flow separation plays a more important role than the Rn-difference factor, then in principle any propeller that suffers from (laminar) flow separation in a SPT will likely get an unusually low η_R with the ITTC-78 method. So this phenomenon does not necessarily occurs only with low blade area propellers, but instead can happen to other propellers as well.

The 2POT method does bring the η_R back to normal value. The near wall flow on blades will probably be a bit more similar with each other for the POT and the SPT cases if they are run at the same low Rn. Moreover, using a POW curve from a low-Rn POT will have an effect on the intersected J_{Tm} and K_Q. It generally leads to a slightly higher η_R and a higher hull efficiency η_H, a slightly lower J_{Tm} and η_{mo}, and finally a few percent increase of η_D. The consequence of applying the 2POT method can be seen in Table 6. Therefore, the 2POT method might be able to give a more fair performance prediction for the low blade area propellers. However, the previous work by other investigators and SSPA's paint test results find that the near wall flows in the POT and SPT, performed at about the same Rn, show a similarity of laminar flow character, but also reveal some differences in the flow orientation. The high turbulence intensity in ship wake has probably made the flow to be more transitional and turbulent. This means if a 2POT method is to be adopted, a somewhat higher Rn than that used in SPT should be chosen for use in the low Rn POT test, in order to achieve some consistency in near wall flow between the two tests. This calls for a thorough calibration work, similar to that being conducted at HSVA (Lücke and Streckwall, 2017).

On the other hand, we have to be aware the disadvantages in model testing with the 2POT method. For example, it can be troublesome to do model test in laminar and transitional flow regimes, as this type of flow is very sensitive to change of model speed (hence Rn number) which sets a very high requirement on the accuracy of the model speed; Laminar flow is vulnerable to free-stream turbulence disturbance and prone to separation. Testing in laminar/transitional flow regime may result in flow instability and oscillating forces, and requires special equipment to reliably measure the forces. Therefore it is preferable not to perform a model test in the low Rn range (unavoidable for SPT). This was one of the reasons to require that a POT be performed at a Rn higher than Rnc when the ITTC-78 method was developed. The challenge that ITTC members are facing is whether a better scaling method or a modified ITTC-78 method, can be developed for non-conventional propellers in future.

6 CONCLUSIONS

In this work model testing and a RANS method with the intermittency transition γ-model were used to study the near-wall flow characters in open water and behind conditions for three propellers, representing a modern low blade area design (Prop A) and two conventional designs (Prop B and C).

For the open water tests at low Rn, the paint test results show clearly a laminar flow dominance on blades for all the propellers. Separation is observed on the SS of Prop A and B. In the high Rn POT, the near wall flow is a combination of laminar, transitional and turbulent flow. There is no separation on the SS of Prop B and C. It is unclear if separation has taken place on the SS of Prop A.

In behind condition, the paint tests show that the flow is mainly a combination of laminar and transitional flow, but the amount of transitional flow has increased. No separation occurs on Prop B and C. It is unclear from the paint test if

there is a separation on the SS of Prop A, but the CFD result predicts a flow separation for this propeller. SSPA's paint test results showed a similar tendency as observed at HSVA w.r.t the different response of the Rn difference in POT and SPT tests for the low and high blade area propellers.

We observe that two factors may have led to the drop of η_R for low blade area propellers. (a) A moderate difference in Rn between the POT (following standard ITTC-78) and SPT that causes a small difference in POW curves; (b) The flow separation on the SS of the blade near T.E. Both factors are related to the design philosophy like chordwise load distribution, thickness-to-chord-ratio, blade section profile and blade area etc. If the flow separation plays a key role, the drop of η_R may also happen to other propellers that suffer from flow separation in a SPT.

The 2POT method offers a solution to the too-low η_R problem and seems to give a fair prediction for low blade area propellers, as it attempts to make the inflow condition (Rn) in a POT consistent with that in a SPT. If an unusual drop of η_R is observed in a prediction with the ITTC-78 method, the 2POT method may be considered as an alternative performance prediction method for propellers that suffer from the η_R problem. With the awareness of the potential problems with the 2POT method (discussed in §5.5), we encourage the continuing effort in the ITTC Committees and member society to develop new scaling methods for unconventional propellers.

The limiting streamlines predicted by the γ-model do not always agree well with the paint test results in the computed cases. An overpredicted laminar zone and delayed transition onset are observed for Prop A in the high Rn case, for Prop B in the low Rn case, and for Prop C at both Rn numbers. The inconsistency in streamline prediction is partially associated with the sensitivity of the transition model to the free-stream turbulence quantities at the inlet, and partly caused by numerical errors. The latter issue will be discussed in a separate paper. Overall, the streamlines predicted by the γ-model have slightly better agreement with the paint tests compared with the SST model in the low Rn cases. Using the turbulence intermittency threshold value as an indicator, the amount of laminar flow area on blade surfaces can be quantified approximately with the γ-model. This information confirms the laminar flow dominance on blades for all propellers at low Rn.

Paint test is still the most reliable and efficient method to detect the presence of laminar and turbulent flow, the onset of transition as well as the occurrence of flow separation. One future work is to study the near wall flow with the present method for propeller with other section profiles, for example, an Eppler-like section. Transition models are known to be sensitive to *Tu* and *TVR* prescribed at the velocity inlet boundary. Without the correct info of *Tu* and *TVR* at some distance upstream the propeller L.E., it is not easy for a transition model in its present form to accurately predict the onset of transition and skin friction at a low Rn.

7 ACKNOWLEDGMENTS

The permission by Nakashima Propeller Co. Ltd. to use their propeller in the study is gratefully acknowledged. The work was funded by the "Hugo Hammars fond för sjöfartsteknisk forskning" and "Fru Martina Lundgrens fond för sjöfartsteknisk forskning" at SSPA.

REFERENCES

Amadeo, M.G., Juan G.A., Marino, P.S. and Leo, G.G. (2017). "Open Water results comparison for three propellers with transition model, applying crossflow effect, and its comparison with experimental results". The 5th International Symposium on Marine Propulsors, SMP'17, Espoo, Finland.

Baltazar, J., Rijpkema, D. and Falcao de Campos, J.A.C. (2017). "On the use of the γ-Re_θ transition model for the prediction of propeller performance at model-scale". The 5th International Symposium on Marine Propulsors, SMP'17, Espoo, Finland.

Bhattacharyya, A., Neitzel, J.C., Steen, S., Abdel-Maksoud, M. and Krasilnikov, V. (2015). "Influence of Flow Transition on Open and Ducted Propeller Characteristics". The 4th International Symposium on Marine Propulsors, SMP'15, Texas, USA.

Bhattacharyya, A., Krasilnikov, V. and Steen, S. (2016a). "A CFD-based scaling approach for ducted propellers". Ocean Engineering 123 (2016) 116–130.

Bhattacharyya, A., Krasilnikov, V. and Steen, S. (2016b). "Scale effects on open water characteristics of a controllable pitch propeller working within different duct designs". Ocean Engineering 112 (2016) 226–242.

Colonia, S., Leble, V., Steijl, R. and Barakos, G. 2017. "Assessment and Calibration of the g-Equation Transition Model at Low Mach", AIAA Journal, Vol.55, No.4, April 2017.

Helma S. (2015) "An Extrapolation Method Suitable for Scaling of Propellers of any Design", The 4th International Symposium on Marine Propulsors, SMP'15, Texas, USA.

Hasuike,N., Okazaki,A. Yamasaki, S. and Ando,J. (2013). "Reynolds effect on Propulsive Performance of Marine Propeller operating in wake flow", Proceedings of 16th NuTTS 2013, Mulheim, Germany.

Hasuike, N., Okazaki, M. and Okazaki, A. (2016). "Flow characteristics around marine propellers in self-propulsion test condition", Proceedings of 19th NuTTS, St. Pierre d'Oleron, France.

Hasuike,N., Okazaki,M., Okazaki A. and Fujiyama, K. (2017). "Scale effects of marine propellers in POT and self-propulsion test conditions". The 5th International

Symposium on Marine Propulsors, SMP'17, Espoo, Finland.

Lopes, R., Eca, L. and Vaz, G. (2017). "On the Decay of Free-stream Turbulence Predicted by Two-equation Eddy-viscosity Models", Proceedings of 20th NuTTS, Wageningen, The Netherlands.

Lücke, T. and Streckwall, H. (2017). "Experience with Small Blade Area Propeller Performance". The 5th International Symposium on Marine Propulsors, SMP'17, Espoo, Finland.

Menter, F.R.(1994). "Two-Equation Eddy-Viscosity Turbulence Models for Engineering Applications", AIAA Journal, 32(8):1598-1605.

Menter, F. R., Smirnov, P. E., Liu, T., and Avancha, R. (2015). "A one-equation local correlation-based transition model". Flow, Turbulence and Combustion, 95(4):583-619.

Streckwall, H., Lucke, T, Bugalski T., Felicjancik J., Goedicke T., Greitsch L., Talay A. and Alvar M. (2016). "Numerical Studies on Propellers in Open Water and behind Hulls aiming to support the Evaluation of Propulsion Tests". Proceedings of 19th NuTTS, St. Pierre d'Oleron, France.

Rijpkema, D., Baltazar, J. and Campos, J.F. (2017). "On the Use of the γ-Re_θ Transition Model for the Prediction of the Propeller Performance at Model-Scale". The 5th International Symposium on Marine Propulsors, SMP'17, Espoo, Finland.

Sánchez-Caja, A., González-Adalid, J., Pérez-Sobrino, M. & Sipilä, T. (2014). "Scale Effects on Tip Loaded Propeller Performance Using a RANSE Solver", Ocean Engineering 88, pp.607-617.

Shin, K.W. and Andersen, P. (2017). "CFD Analysis of Scale Effects on Conventional and Tip-Modified Propellers". The 5th International Symposium on Marine Propulsors, SMP'17, Espoo, Finland.

Tamura, K. and Sasajima, T. (1977). "Some investigations on propeller open-water characteristics for analysis of self-propulsion factors", MTB 119, March 1977.

Tsuda, T., Konishi, S., Asano, S., Ogawa, K. and Hayasaki, K. (1978). "Effect of propeller Reynolds number on self-propulsion performance", Japan Society of Naval Architects and Ocean Engineering, Vol 169.